

RI 9213

RI 9213

REPORT OF INVESTIGATIONS/1989

# Fe-Ni-Cr Alloys for Coatings and Electroforms

By J. E. Allison, Jr., and G. R. Smith

BUREAU OF MINES



UNITED STATES DEPARTMENT OF THE INTERIOR

**Report of Investigations 9213**

# **Fe-Ni-Cr Alloys for Coatings and Electroforms**

**By J. E. Allison, Jr., and G. R. Smith**

**UNITED STATES DEPARTMENT OF THE INTERIOR  
Donald Paul Hodel, Secretary**

**BUREAU OF MINES  
T S Ary, Director**

**Library of Congress Cataloging in Publication Data:** \_\_\_\_\_

**Allison, J. E.**

Fe-Ni-Cr alloys for coatings and electroforms.

(Bureau of Mines Report of investigations; 9213)

Bibliography: p. 13.

Supt. of Docs.: I28.23:9213.

1. Chromium-iron-nickel alloys. 2. Alloy plating. 3. Electroforming. I. Smith, Gerald R., 1942- . II. Title. III. Series: Report of investigations (United States. Bureau of Mines); 9213.

TN23.U43

[TN757.N6]

622 s [671.7]

88-600301

## CONTENTS

Page

Abstract .....	1
Introduction .....	2
Experimental Work .....	2
Electrolytic cell .....	2
Electrodeposited composite material .....	3
Characterization .....	3
Heat treatment .....	3
Alloy coatings and electroforms .....	3
Properties .....	3
Corrosion-resistance tests .....	4
Results and discussion .....	4
Preparation of composite coatings .....	4
Powder suspension .....	4
Matrix composition and microstructure .....	5
Surface-active agents .....	7
Properties of heat-treated coating .....	8
Grain size .....	8
Homogeneity and porosity .....	8
Interface characteristics .....	8
Hardness and ductility .....	11
Corrosion resistance of coating .....	11
Heat-treatment effects .....	11
Protection of carbon steel .....	11
Electroforms .....	11
Conclusions .....	12
References .....	13

## ILLUSTRATIONS

1. Schematic of electroplating assembly .....	2
2. Size distribution of Cr particles suspended in electrolyte, determined by Coulter counter particle analyzer .....	3
3. Relationship between Cr powder suspended in electrolyte and occluded in coating .....	5
4. Schematic model of occlusion process proposed by Guglielmi .....	6
5. Plot of suspended particles per occluded particles versus suspended particles .....	6
6. Effects of Fe-Ni matrix composition and microstructure on occlusion of Cr particles .....	7
7. Effect of surface-active agents on occlusion of Cr particles .....	7
8. Cross-sectional microstructure of heat-treated stainless steel coating .....	8
9. Cross-sectional photomicrographs and EDX (for Cr) before and after heat treatment .....	9
10. Effect of Ni undercoat on carbon diffusion .....	10
11. Microprobe trace of heat-treated coating .....	10
12. Fe-Ni-Cr alloy coating after exposure to HNO <sub>3</sub> solution .....	12
13. Heat-treated Fe-Ni-Cr alloy electroforms .....	12
14. Polished Fe-Ni-Cr alloy electroforms .....	12

## TABLES

	<i>Page</i>
1. Electrolyte composition .....	3
2. Chromium particles suspended, loosely adsorbed, and occluded at 10 A/dm <sup>2</sup> .....	6
3. Cross-sectional microhardness and microstructure of Fe-Ni-Cr alloy coatings .....	11
4. Effects of heat-treatment time and furnace pressure on coating homogenization .....	12

### UNIT OF MEASURE ABBREVIATIONS USED IN THIS REPORT

A/dm <sup>2</sup>	ampere per square decimeter	μm	micrometer
°C	degree Celsius	mm/yr	millimeter per year
°C/h	degree Celsius per hour	mol/L	mol per liter
cm	centimeter	pct	percent
dm <sup>2</sup>	square decimeter	ppm	part per million
DPH	diamond pyramid hardness	rpm	revolution per minute
g/cm <sup>3</sup>	gram per cubic centimeter	s	second
g/L	gram per liter	Torr	torr
h	hour	vol pct	volume percent
mL	milliliter	W	watt
mm	millimeter	wt pct	weight percent

# Fe-Ni-Cr ALLOYS FOR COATINGS AND ELECTROFORMS

By J. E. Allison, Jr.,<sup>1</sup> and G. R. Smith<sup>2</sup>

---

## ABSTRACT

As part of a Bureau of Mines research program to conserve critical and strategic metals, an aqueous electrodeposition method for preparing stainless-steel-type coatings was studied. Chromium powder (averaging 3  $\mu\text{m}$  diam) was suspended in a ferrous-nickelous sulfate electroplating bath and occluded in the electrodeposited Fe-Ni alloy matrix. Subsequent heat treatment of the resulting composite coating formed the ternary alloy.

The occlusion process was affected by the quantity of Cr powder suspended in the electrolyte and by the microstructure and composition of the electrodeposited matrix. Coatings containing up to 21 wt pct Cr were deposited from an electrolyte containing 20 vol pct suspended Cr powder. Heat treatment at 1,100° C for 8 h homogenized the composite coating. Deposition of 44Fe36Ni20Cr alloy coatings (250  $\mu\text{m}$  thick) on AISI 1020 carbon steel rods, followed by heat treatment, provided complete protection of the carbon steel during exposure to a boiling 65-pct-HNO<sub>3</sub> solution. Corrosion rates of 0.6±0.4 mm/yr for the coating in the boiling HNO<sub>3</sub> approximate that of 304 stainless steel. Practically shaped electroforms have been prepared by the coating method.

---

<sup>1</sup>Metallurgist, Albany Research Center, Bureau of Mines, Albany, OR (now with Naval Sea Systems Command, U.S. Navy, Crystal City, VA).

<sup>2</sup>Physical scientist, Division of Mineral Commodities, Branch of Ferrous Metals, Bureau of Mines, Washington, DC.

## INTRODUCTION

It has been known for many years that insoluble particles suspended in an electrolyte during plating can be occluded in the electrodeposited metal. In recent years, particle-occlusion methods have been used advantageously to produce a variety of electrodeposited composite coatings (1-3).<sup>3</sup> These metal-matrix composites have contained powders and fibers, including oxides (4-9), nitrides (3), carbides (10-11), diamonds (12-13), and graphite (1), that have improved the oxidation (4,14), corrosion (15), or wear resistance (3, 16-18) of the electrodeposits, increased their strength (4, 19-21), or imparted a decorative (22) or lubricative (3, 23) quality to them. Because-Cr bearing alloys electroplated by conventional processes are thin and highly stressed and can be produced only at low efficiencies, particle-occlusion methods have been considered as an alternative method of introducing Cr in an alloy coating. In this procedure, metal powder is occluded in an electrodeposited metal matrix and heat treated to form an alloy. Bazzard and Boden (24-25) reported on preparing Ni-Cr

alloy coatings by occluding Cr powder in a Ni matrix and then heat-treating at 800° to 1,050° C. Kilgore (26) and Williams (27) suggested that a particle-occlusion method could be used to produce stainless steel coatings, but their reports did not contain experimental results. Research conducted by the Bureau of Mines (28-29), however, has provided experimental evidence of the feasibility of this method.

This report presents results of experiments conducted to produce stainless-steel-type Fe-Ni-Cr alloy coatings and electroforms using the particle-occlusion, heat-treatment method. It addresses the effects of several electrolytic cell parameters on the quantity of Cr particles occluded in the composite coatings. Included also are discussions on the properties of the pre- and post-heat-treated coatings as well as the effectiveness of the heat-treatment procedures to homogenize the composite coating into a corrosion-resistant ternary alloy. Adaptability of the method to preparing thick electroforms is also discussed.

## EXPERIMENTAL WORK

### ELECTROLYTIC CELL

A 100-mm-diam and 135-mm-high polymethylmethacrylate plating cell (fig. 1), was used to prepare the composite coatings. Two Ni anodes and two Fe anodes, 99.9 and 99.6 pct pure, respectively, were positioned equidistant around the cathode. In the experiments conducted to establish electrodeposition and heat-treatment conditions required to produce a corrosion-resistant Fe-Ni-Cr alloy, the composite coating was electrodeposited on a cold-drawn 10-mm-diam AISI 1020 carbon steel rod, which had been sanded with a 240-grit paper and which had an effective plating area of 0.13 dm<sup>2</sup>. In the experiments on preparing Fe-Ni-Cr alloy electroforms, the cathode material was a 60Sn40Bi alloy mandrel, melted and cast to a prescribed shape and polished with 600-grit paper. Several mandrel shapes were used ranging in area from 0.13 to 0.38 dm<sup>2</sup>.

The cathode was rotated at 1 rpm during electrolysis. Current to the cell was controlled by two dc power supplies connected in parallel. This permitted independent control of the current passing through the Fe and Ni anodes, which made it possible to match dissolution rates with deposition rates to maintain a more consistent electrolyte composition. Total charge passed through the cell was recorded with an ampere-hour meter. Temperature of the electrolyte was controlled at 70° C using a proportional temperature controller and a 400-W quartz-sheathed immersion heater. The pH was regulated between 2.1 and

2.3 with an automated pH controller by periodic additions of 10-pet H<sub>2</sub>SO<sub>4</sub>.

The electrolytes were prepared with hydrated metal salts and deionized water. Their general composition is listed in table 1. Although the electrolytes were prepared

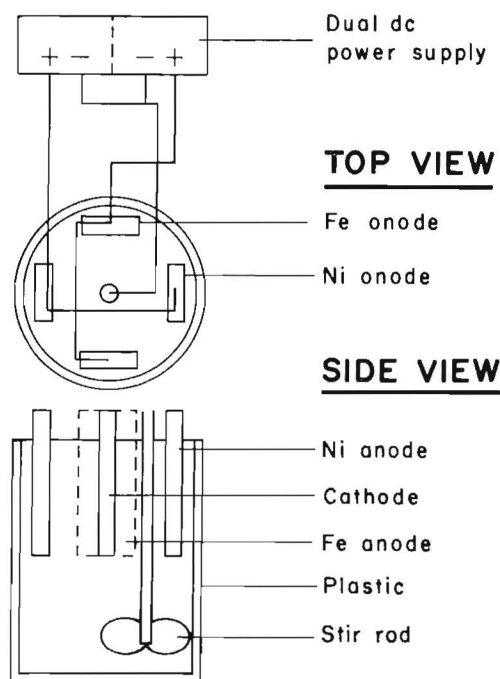


Figure 1.—Schematic of electroplating assembly.

<sup>3</sup>Italic numbers in parentheses refer to items in the list of references at the end of this report.

**Table 1.—Electrolyte composition**

Constituent	Conc, mol/L
Reducible ions (Fe <sup>2+</sup> , Ni <sup>2+</sup> )	1.78
Sulfate ion	1.67
Chloride ion	.11
Boric acid	.65
Sodium saccharin	.04

with a total metal ion concentration of 1.78 mol/L, the relative ratio of ferrous (Fe<sup>2+</sup>) and nickelous (Ni<sup>2+</sup>) ions in the electrolytes was varied to change the ratio of Fe and Ni in the electrodeposits. Sodium saccharin was added to relieve internal stresses in the electrodeposit; boric acid was added as a buffer; and chloride ions were used to prevent passivation of the Ni anodes.

The Cr powder was suspended in the electrolyte by stirring at 360 rpm with a polypropylene propeller, 50-mm diam, positioned near the base of the cell. The concentration of Cr powder suspended is reported in volume percent. The weight of Cr powder was calculated using a density of 7.2 g/cm<sup>3</sup>. Chromium powder was added to the plating cell, and the total volume was adjusted with electrolyte. One hundred percent of the powder was assumed to be suspended.

Commercially available Cr powder (99.86 pct Cr, ≈0.02 pct C) was used to prepare the composite coatings. The particle size, ≈3μm, was determined (fig. 2) using a Coulter<sup>4</sup> counter particle analyzer. Particles in 16 size ranges from 0.8 to 24 μm were electronically counted and the numbers converted to volume percent using the particle count and average particle size for each size range. The particles were also examined with a transmission electron microscope and found to be predominantly spherical in shape.

## ELECTRODEPOSITED COMPOSITE MATERIAL

### Characterization

The electrodeposited metal and the occluded powder content of the composite coating were determined by two techniques. In the first technique, the coating was physically removed from the steel cathode or the electroform was separated from the Sn-Bi mandrel by melting the mandrel at ≈170° C. The composite was then dissolved in a 10-pct-HNO<sub>3</sub> solution and filtered to recover insoluble Cr particles. Subsequently, the Fe and Ni were determined either by atomic absorption (AA) or inductively coupled plasma emission spectroscopy (ICP). In the second technique, the composite was analyzed directly on the cathode with an alloy analyzer that uses radioisotope (Fe-55 or Cd-109) excited X-ray fluorescence to determine composition. The alloy analyzer was accurate within ±1.5 wt pct for Cr and ±3 wt pct for Fe and Ni. X-ray diffraction methods were used to identify the phases

<sup>4</sup>Reference to specific products is made for identification only and does not imply endorsement by the Bureau of Mines.

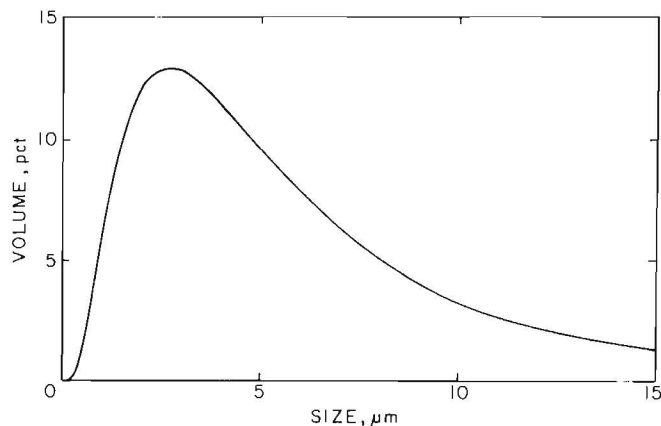


Figure 2.—Size distribution of Cr particles suspended in electrolyte, determined by Coulter counter particle analyzer.

of the composites. Scanning electron microscopy (SEM) and energy dispersive X-ray analysis (EDX) were used to examine the distribution of the Cr powder within the electrodeposited matrix. Image analysis was performed using SEM with an automated image analyzer.

### Heat Treatment

The electrodeposited composite was heat treated at 1,100° C in a vacuum furnace, using a heating rate of 60° to 120° C/h. The furnace was evacuated to 10<sup>-6</sup> Torr during the heat treatment. After heat treatment, the samples were allowed to cool in the furnace at a typical rate of ≈1,000° C/h. Each sample was reheated to 1,100° C under a nitrogen atmosphere for 1 h, removed from the furnace, and then quenched in still water to prevent segregation of carbides and possible formation of detrimental phases (for example, brittle sigma phase).

## ALLOY COATINGS AND ELECTROFORMS

### Properties

Chemical and mechanical properties of the heat-treated coatings and electroforms were determined by the following methods.

Electron microprobe and EDX procedures were used to examine interdiffusion at the interface of the 1020 steel substrate and the alloy coating and to evaluate the effects of an electrodeposited Ni barrier on this interdiffusion. Prior to deposition of the Ni barrier from a conventional Watts- or Woods-type electrolyte, the steel substrate was cleaned in 10-pct-HNO<sub>3</sub> and 25-pct-HCl solutions. After Ni deposition, the composite coating was immediately deposited onto the Ni barrier.

Adhesive properties of the Fe-Ni-Cr alloy coating were evaluated by a qualitative bend test method (ASTM B571-79). In this method, the coating was deposited over a 7-cm length of Ni-precoated carbon steel strip (2.5 cm wide by 0.16 cm thick) and bent around a rod having a diameter four times the thickness of the strip plus coating. Examination of the deformed area under low-power magnification provided no evidence of peeling or flaking from the substrate.

Another bend test (ASTM B489-68) was used to measure the ductility of the Fe-Ni-Cr alloy. Strips of 45Fe36Ni19Cr alloy coating (7.0 cm long by 2.5 cm wide by 0.05 cm thick), prepared by heat treating Fe-Ni-Cr powder composite electroforms, were used as test specimens. The ductility, that is, the percent elongation before fracture, was determined by bending the strips around progressively smaller diameter rods.

Microhardness numbers were obtained for cross sections of the alloy coatings and electroforms using a Vickers microhardness tester. In preparation for these measurements, the cross sections were ground with 600-grit paper, then polished with 6- $\mu\text{m}$  diamond and 2- $\mu\text{m}$  cerium oxide powders.

Grain size within the alloy microstructure was determined by employing the Heyn procedure described in ASTM standard E112-82. This line-intercept method uses a count of the grain boundaries intersected per millimeter length of straight line to estimate the ASTM grain-size number. An electrolytic etch for 30 s in cupric sulfate solution (50 g/L) revealed the grain structure of the alloy.

Alloy porosity was determined from an SEM image of the cross section. An average count and the dimension of voids per unit area were obtained with a computerized image analyzer. Grinding and polishing steps were carefully controlled to minimize the creation of false voids associated with the loss of undissolved phases such as carbides or hard FeCr phases. In these preparation steps

napless cloth and alcohol-based lubricant were used. The surface was ground with 320-grit paper, then polished with 6- $\mu\text{m}$  and 1- $\mu\text{m}$  diamond powders.

### Corrosion-Resistance Tests

Three types of test specimens were prepared for determining the corrosion resistance of the heat-treated Fe-Ni-Cr alloys. The first type was an electrodeposited composite coating that had been physically removed from the carbon steel substrate prior to heat treatment. In this form, corrosion resistance of the coating served as a standard for evaluating the effectiveness of the various heat-treatment procedures used to homogenize the coatings. This evaluation could be done without considering adverse effects caused by coating-substrate interactions. The second specimen type had a substrate that was composed of a carbon steel rod mechanically joined with a 304 stainless steel rod cap on the end that extended out of the electrolyte. The Ni barrier and composite coatings bridged the surface between the cap and the carbon steel rod. Because the carbon steel was effectively encapsulated with corrosion-resistant material, it was possible to evaluate the overall protective quality of the heat-treated coating. An electroetch (60 s in a 5-pct- $\text{H}_2\text{SO}_4$  solution) was used to activate the stainless steel cap for electrodeposition of the Ni barrier. The third type of specimen was an electroformed shape from which the Sn-Bi mandrel was removed by melting prior to heat treatment. Corrosion resistance of freestanding, thick, and intricately shaped alloys was determined with the electroformed shapes.

Test specimens were exposed to a boiling 65-pct- $\text{HNO}_3$  solution for as many as five 48-h stages, the standard corrosion test for chromium segregation in commercial stainless steels (Huey test).

## RESULTS AND DISCUSSION

### PREPARATION OF COMPOSITE COATINGS

The first step in producing an Fe-Ni-Cr alloy coating was electrodeposition of a metal-metal composite coating consisting of an Fe-Ni matrix with occluded Cr powder. To consistently produce good coatings, it was necessary to establish those factors that would affect the occlusion process. Amount of suspended Cr powder, current density, composition of the electrolyte, and presence of surface-active agents were found to be the most important factors affecting the occlusion of particles. Temperature (50° to 70° C), pH (1.5 to 2.3), and total concentration of reducible ions (1.34 to 1.78 mol/L) did not significantly affect the amount of Cr powder occluded.

### Powder Suspension

To determine the relationship between the concentration of Cr particles suspended and the quantity of particles occluded, the Cr suspension was varied from 0.3 to 30 vol pct and electrodeposits were prepared at 2.5 and 10 A/dm<sup>2</sup>. The Cr was occluded into an 86Fe14Ni electrodeposit from an electrolyte containing 1.068 mol/L  $\text{Fe}^{2+}$  and 0.712 mol/L  $\text{Ni}^{2+}$ .

Figure 3 shows that the percentage of Cr in the composite coatings increased significantly as the concentration of suspended Cr powder was increased above 1 or 2 vol pct. These data are consistent with a model

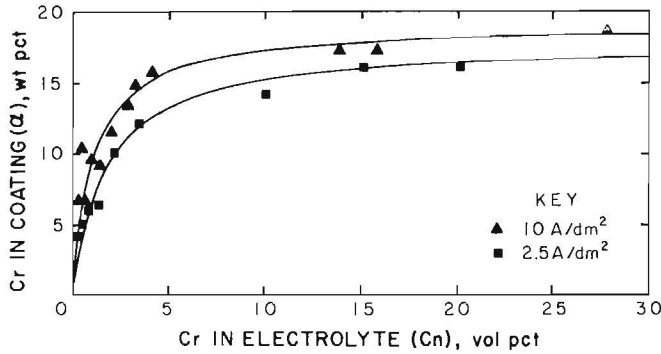


Figure 3.—Relationship between Cr powder suspended in electrolyte and occluded in coating.

proposed by Guglielmi (5) for the occlusion of ceramic particles in an electrodeposited Ni matrix. The model shown schematically in figure 4 consists of a two-step mechanism in which particles are loosely adsorbed on the cathode surface and then strongly adsorbed by a field-assisted mechanism and occluded into the electrodeposit.

This adsorption of the suspended particles is postulated to obey a model analogous to the Langmuir isotherm and to depend on the concentration of suspended particles in accordance with the expression

$$\sigma = \frac{KCn}{1 + KCn} (1 - \theta), \quad (1)$$

where  $\sigma$  = loose-adsorption coverage,

$\theta$  = strong-adsorption coverage,

$Cn$  = concentration of suspended particles, vol pct,

and  $K$  = constant that depends on interaction between Cr particles and cathode surface.

If it is assumed that every particle that is strongly adsorbed becomes occluded, then  $\theta$  will equal the volume fraction of particles in the coating ( $\alpha$ ), provided that the two-dimensional area projection for the particle is approximately equal to the volume fraction.

Guglielmi (5) further related the volume fraction of occluded particles to the concentration of particles in solution,

$$(1 - \alpha) \frac{Cn}{\alpha} = [\text{constant}] \left( \frac{1}{K} + Cn \right). \quad (2)$$

The constant contains a term for the current density of the metal deposition process. In the case of Fe-Ni alloy deposition, this term is proportional to the sum of the two partial reduction currents for Fe and Ni.

The K-constant can be estimated from the slope and intercept of these lines [ $K$  = slope + intercept]. Data from figure 3 plotted in this manner (fig. 5) were linear and agreed with the model. The plots gave values of  $K = 0.7 \pm 0.1$  and  $0.5 \pm 0.1$  for 2.5 and 10 A/dm<sup>2</sup>, respectively. Since different Fe-Ni alloy compositions are formed at each current density, the K-value may change with current density. K-values between 2.8 and 8.3 have been reported for the occlusion of ceramic particles in a single metal matrix (5, 30). The lower K-values reported here indicate that Cr has less of a tendency to loosely adsorb on the cathode surface than do ceramic particles.

Data presented in table 2 show the percent loose-adsorption coverage of Cr particles ( $\sigma$ ) derived from equation 1, the volume of suspended Cr particles required to achieve this coverage ( $Cn$ ) and the resulting percentage of Cr powder occluded in the deposit ( $\alpha$ ). The volume fraction of particles in the deposit ( $\alpha$ ) has been used to estimate the strong adsorption coverage ( $\theta$ ).

When these data are compared with Guglielmi's data from ceramic powders, ceramic powders are found to be more readily adsorbed on the cathode surface. Once the particles are loosely adsorbed, however, Cr particles are more readily occluded into the electrodeposit. Guglielmi (5) has reported that a suspension of 0.78 vol pct TiO<sub>2</sub> particles was required to obtain a loose-adsorption coverage of 75.5 pct and to occlude 6.2 vol pct particles in the electrodeposit. Silicon carbide was also reported to require only 0.31 vol pct suspended powder to obtain a loose-adsorption coverage of 75.5 pct and a total occlusion of 2.1 vol pct particles. Chromium powder required more suspended particles ( $Cn = 20.14$  vol pct) to obtain a comparable loose-adsorption coverage ( $\sigma = 75.2$  pct), but a greater occlusion of Cr particles ( $\alpha = 17.26$  vol pct) was obtained.

### Matrix Composition and Microstructure

When the Fe-Ni-Cr particle composite is electrodeposited, the microstructural characteristics vary depending upon its composition. According to Fedorova (31), a single-phase gamma (Ni,Fe) structure is obtained for electrodeposits containing <47 wt pct Fe, and a single-phase alpha (Fe,Ni) structure is obtained for electrodeposits containing >81 wt pct Fe. A mixed structure exists between these compositions. X-ray diffraction data for the composite coatings prepared at 2 A/dm<sup>2</sup> showed that the microstructure of the coatings was consistent with Fedorova's results.

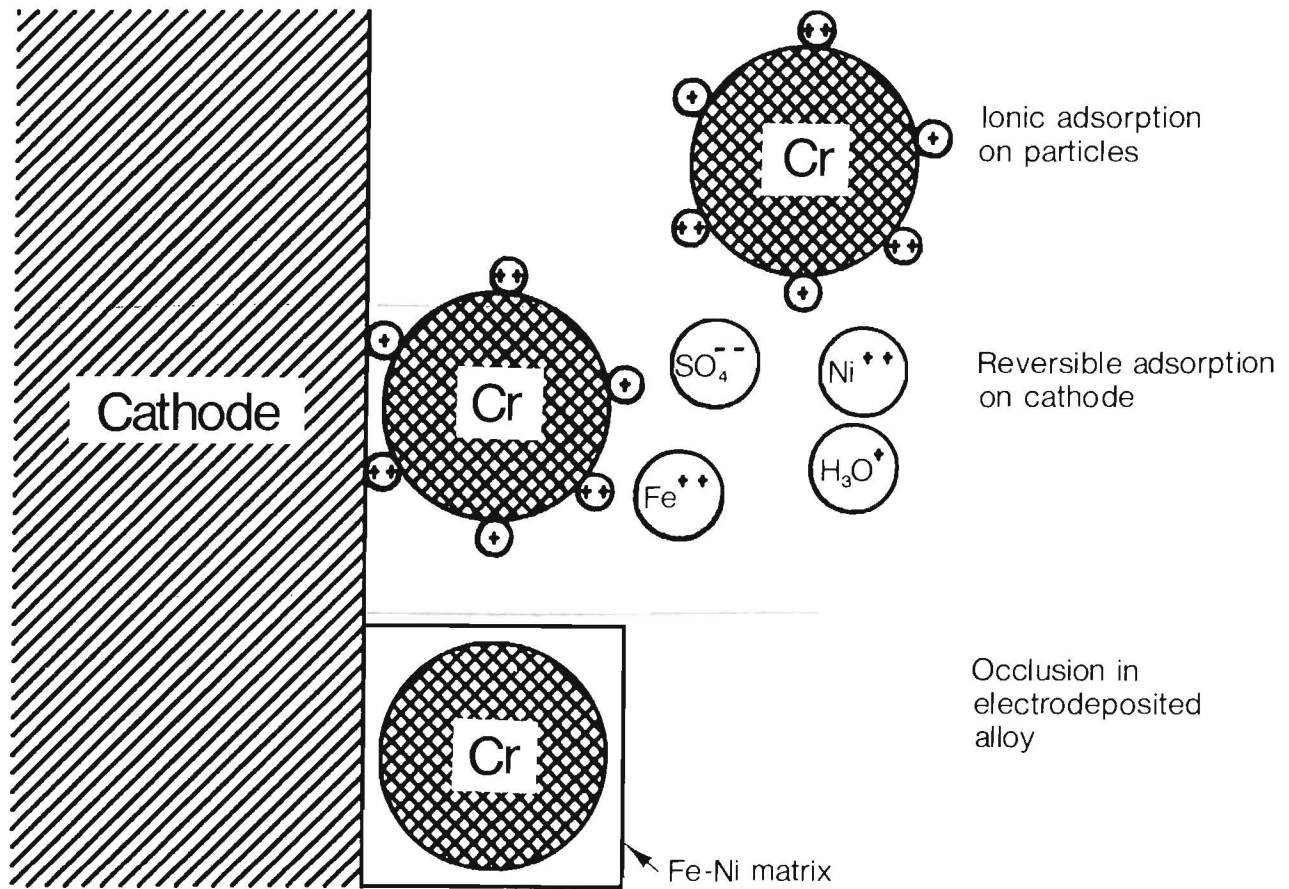


Figure 4.—Schematic model of occlusion process proposed by Guglielmi (5).

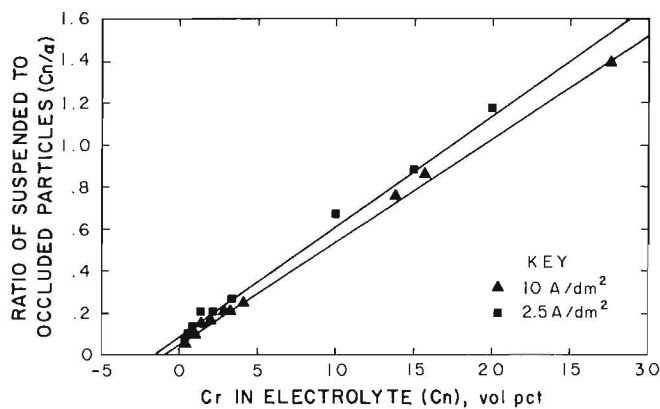


Figure 5.—Plot of suspended particles per occluded particles versus suspended particles.

Table 2.—Chromium particles suspended, loosely adsorbed, and occluded at 10 A/dm<sup>2</sup>

Suspended (Cn), vol pct	Loosely adsorbed (σ), pct	Occluded (α), vol pct
0.35	14.9	4.46
.88	28.5	6.46
2.19	46.7	10.58
10.07	70.7	15.18
20.14	75.2	17.26

To establish the relationship between the current density, the matrix composition, the microstructure, and the quantity of Cr particles occluded, electrolytic experiments were conducted at total current densities (sum of H, Fe, and Ni) of 2, 5, and 10 A/dm<sup>2</sup> over the full range of matrix composition (fig. 6). Using a 20-vol-pct Cr particle suspension to ensure maximum availability of suspended Cr particles at the electrode surface, the amount of Cr occluded increased as the Fe in the gamma (Ni,Fe) matrix

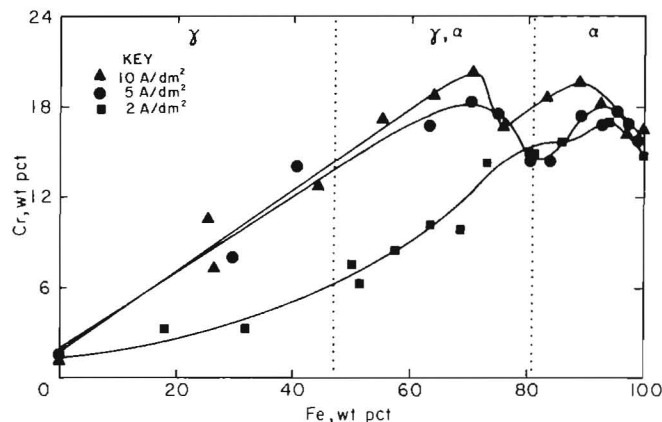


Figure 6.—Effects of Fe-Ni matrix composition and microstructure on occlusion of Cr particles.

increased. The largest quantities of Cr particles were occluded when the electrolytic conditions yielded either a mixed or an alpha (Fe,Ni) microstructure. The relationship between Cr particle occlusion and matrix composition may be influenced by the number of cations adsorbed on the particle surface from the electrolytes used or by the compatibility of the particle and matrix lattice structures. When a gamma (Ni,Fe) structure is plated, most of the cations that are reduced are nickelous ions. An order of magnitude fewer Cr particles is occluded from a  $\text{NiSO}_4$  plating bath than from a  $\text{FeSO}_4$  plating bath.

In general, the percentage of Cr occluded in a matrix composition increased as the current density increased. This trend is consistent with particle occlusion for other metal particle systems when the metal is being deposited under activation overvoltage control conditions (30).

### Surface-Active Agents

Surface-active agents are commonly used in electrolytes to reduce pitting and as leveling or brightening agents (16). Typically, such agents in the ferrous-nickelous sulfate and Cr powder electrolyte yielded smoother composite coatings with fewer voids. Both cationic (alkyl sulfide trimethylammonium halides) and anionic (sodium-2-ethylhexyl sulfosuccinate) surface-active agents were effective. Besides improving the quality of the electrodeposited composite, the surface-active agents reduced the quantity of Cr particles occluded into the matrix. A series of electrodeposits was made in an electrolyte containing 0.445 mol/L  $\text{Fe}^{2+}$  ions and 1.335 mol/L  $\text{Ni}^{2+}$  at a current density of 5 A/dm<sup>2</sup> and a pH of 2.3. Plots of surface-active agent concentration versus Cr particle occlusion

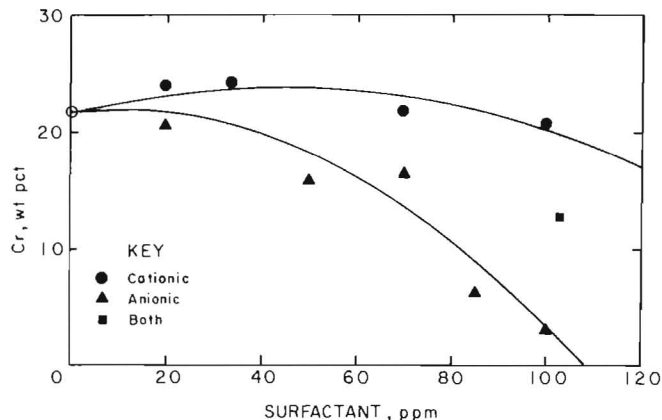


Figure 7.—Effect of surface active agents on occlusion of Cr particles.

(fig. 7) show that additions of the anionic agent suppressed the occlusion of particles. The suppression was slight at concentrations of 20 ppm, but became significant at 100 ppm. At 100 ppm, the Cr content of the composite was 3 wt pct, compared with 21 wt pct at 20 ppm. In comparison, a cationic surface-active agent enhanced the occlusion of particles from  $\approx 21$  to 24 wt pct. The cationic surface-active agent could also be used to counteract the suppression of occlusion caused by the anionic surfactant. For example, an addition of 2.75 ppm cationic surfactant to an electrolyte containing 100 ppm anionic surfactant increased the Cr content of the composite from  $\approx 3$  to 12 wt pct.

These results were consistent with those of other researchers (15, 30) who showed that small amounts of inorganic cations adsorbed on the surface of suspended particles significantly affected the co-deposition process. Anions have also been shown to affect the charge of the particle and the amount of particles occluded (32). Assuming that the cationic and anionic surface-active agents are adsorbed on the surface of the particles and that the occlusion process contains an electric field dependent step (32) related to the actual charge carried by the particles, then any particles containing anionic agent would be expected to be repelled at the cathode and thus be less likely to be occluded into the electrodeposited matrix.

Although cationic agents were effective in producing a low-void coating of high Cr concentration, the distribution of the occluded Cr particles was observed to be significantly less uniform. The subsequent use of a combination of anionic and cationic surface-active agents at 10 to 4 ppm, respectively, repeatedly produced coatings of uniform composition while maintaining deposit quality

and composition. A series of electrodeposits was made in an electrolyte containing 20 vol pct suspended Cr powder, 0.420 mol/L  $\text{Fe}^{2+}$  ions, and 1.360 mol/L  $\text{Ni}^{2+}$  ions at a current density of 5 A/dm<sup>2</sup> and a pH of 2.1. When the tests were done in an electrolyte containing no added surfactants, the average amount of Cr powder occluded was 17 wt pct with a standard deviation of 2-1/2 wt pct. When typical cationic and anionic surface-active agents were used (4 ppm alkyl sulfide trimethylammonium halide and 10 ppm sodium-2-ethylhexyl sulfosuccinate), the average amount of Cr powder occluded was increased to 21.6 wt pct, but the reproducibility was not significantly improved (2 pct).

### PROPERTIES OF HEAT-TREATED COATING

The last step in producing an Fe-Ni-Cr alloy coating was heat-treating the composite coating to dissolve the Cr particles into the Fe-Ni matrix.

Following heat treatment, the Fe-Ni-Cr alloys were examined to determine chemical and mechanical properties and physical characteristics. Grain size, chemical uniformity, porosity, diffusion at the substrate-coating interface, hardness, and ductility were examined.

#### Grain Size

Figure 8 shows the microstructure of a typical coating after heat treatment at 1,100° C for 8 h under vacuum ( $1 \times 10^{-6}$  Torr). Prior to heat treatment, the composite coating was physically separated from the substrate. After heat treatment, an average grain size of 3 to 5  $\mu\text{m}$  diam was observed, representing an ASTM grain size number between 13.5 and 14. An ASTM grain size of 6 is typical for a hot-rolled bar or sheet steel, with grain sizes greater than 12 considered to be fine grained.

The fine grain size in the ternary alloy was believed to be caused by two factors. First, the Cr particles may have acted as nucleation sites for the initiation of many grains. Second, heat treatment caused phase transformations that effectively recrystallized the alloy. For example, the microstructure of the electrodeposited composite, before heat-treating, consisted of Cr particles (bcc) in a mixed gamma-phase (fcc), alpha-phase (bcc) Fe-Ni matrix. During the heat treatment, the alpha-phase in the matrix transformed into gamma-phase. As the Cr particles dissolved into the Fe-Ni matrix, the alpha-phase may have become stable while the Cr concentration was high. This would have induced a transformation from gamma-phase to alpha-phase and then back to the gamma-phase. These transformations would promote nucleation and produce a fine-grained microstructure.

#### Homogeneity and Porosity

During heat treatment, the individual Cr particles were interdiffused with the Fe-Ni matrix to obtain an Fe-Ni-Cr ternary alloy. The photographs in figure 9 show the extent to which the Cr particles were interdiffused in a typical

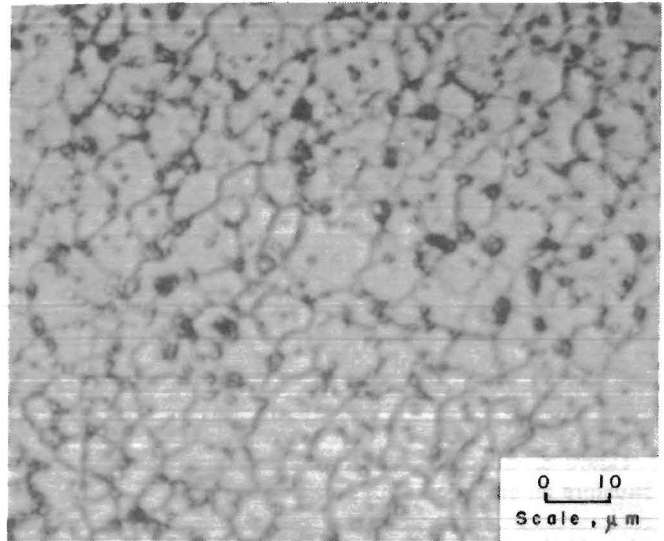


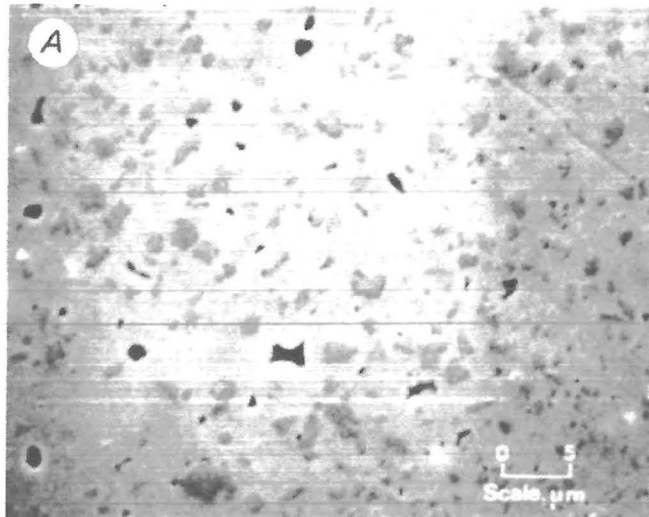
Figure 8.—Cross-sectional microstructure of heat-treated stainless steel coating. The coating has been etched to reveal the grain boundaries.

57Fe20Ni23Cr alloy following heat treatment at 1,100° C for 8 h under vacuum. The SEM photograph of the unhomogenized composite (9A) shows discrete particles distributed throughout the electrodeposited Fe-Ni alloy matrix. An EDX map for Cr at the same locations (9B) shows the occluded particles appearing as bright areas. After heat treatment, significant dispersion of the Cr particles was observed as evidenced by the lack of distinguishable 3- $\mu\text{m}$  particles in the matrix (9C) and the relatively uniform appearance of the associated EDX map for Cr (9D).

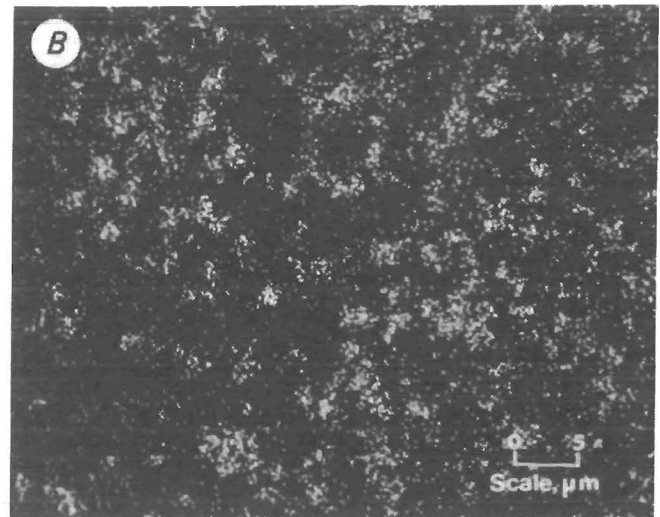
Some porosity was exhibited, however, within this Fe-Ni-Cr alloy following heat treatment, which appears as small, uniformly distributed dark areas in figure 9C. The pores are separated and do not appear to form a network throughout the metal. Pore sizes ranged from 0.01 to 3.0  $\mu\text{m}$  in diameter and accounted for  $\approx 5$  pct of the microstructure. It is believed that the pores are the result of a more rapid diffusion of the Cr particles into the Fe-Ni matrix than of the matrix into the Cr (33).

#### Interface Characteristics

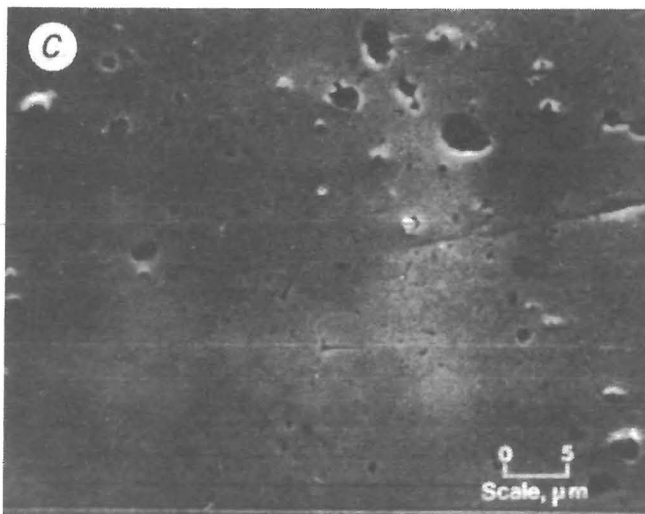
In order to produce a practical, corrosion-resistant coating from an Fe-Ni-Cr powder composite, the heat-treatment steps must be effective in dispersing the Cr throughout the deposit without causing detrimental interaction between the substrate and coating. This interaction may include migration of carbon from the substrate to the coating and subsequent formation of harmful carbides or diffusion of the Fe, Ni, and Cr constituents with the substrate, which results in dilution of the coating composition. In addition, the heat-treatment procedures should produce a coating that adheres to the substrate with a strength equal to that of the substrate and



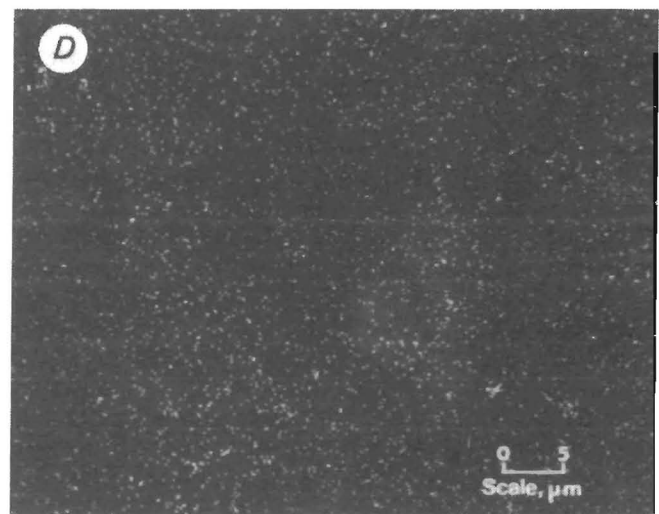
Composite coating



EDX of composite coating



Heat-treated coating



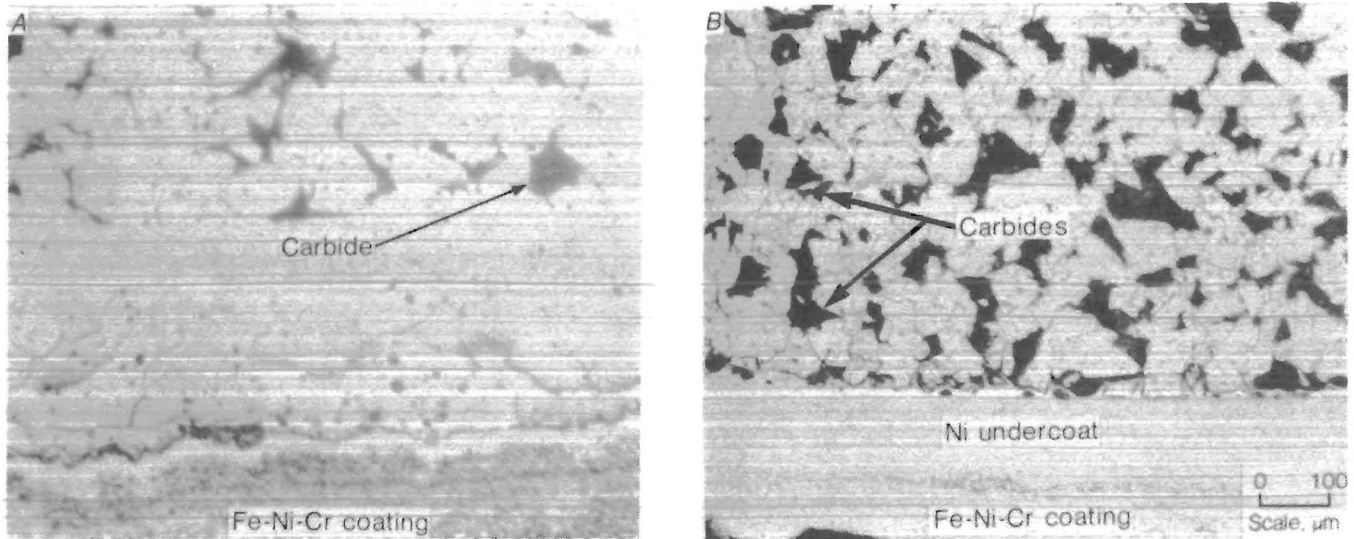
EDX of heat-treated coating

Figure 9.—Cross-sectional photomicrographs and EDX (for Cr) before and after heat treatment, displaying the Cr particles occluded and the effectiveness of the heat treatment in distributing the Cr concentration.

causes little change in the properties of the substrate material.

The coating exhibited an austenitic, stainless-steel-like microstructure after heat treatment. As with conventional austenitic stainless steels, therefore, the coating's corrosion resistance is strongly affected by its carbon content. In the specific case of 304 stainless steel, a significant decrease in corrosion resistance to  $\text{HNO}_3$  is observed when the level of carbon in the metal exceeds 0.2 wt pct. Above this level the alloy cannot be annealed to eliminate sensitization, which causes an increase in localized corrosion at the grain boundaries.

— Experimental results showed that when an Fe-Ni-Cr powder composite was heat treated on a carbon steel substrate at  $1,100^\circ\text{C}$  for 8 h, carbon diffused into the coating, resulting in levels as high as 2 wt pct. A Ni undercoating (diffusion barrier) reduced to tolerable levels the migration of carbon from the substrate to the coating. The effectiveness of the Ni barrier in reducing carbon diffusion is shown in figure 10. Microscopic examination of a heat-treated alloy coating with a  $50\text{-}\mu\text{m}$ -thick electro-deposited Ni diffusion barrier (10B) revealed a significant concentration of pearlite (dark areas) in the substrate up to the Ni barrier-substrate interface and low carbide levels



**Figure 10.**—Effect of Ni undercoat on carbon diffusion from carbon-steel substrate into Fe-Ni-Cr alloy coating. *A*, A pearlite-free zone near the substrate-coating interface is associated with C diffusion from the carbide-containing pearlite in the substrate into the coating; *B*, use of a Ni undercoat retards this diffusion.

in the coating. Similar results were achieved with a 25- $\mu\text{m}$ -thick diffusion barrier. Without the Ni diffusion barrier (10A), carbon diffused from the pearlite into the coating, resulting in a pearlite-free zone at the substrate-coating interface and evidence of significant quantities of carbides in the coating.

The extent of interdiffusion of the Fe, Ni, and Cr during the heat-treatment step was determined by electron microprobe. Figure 11 shows the microprobe profile for Cr and Ni in a sample with a typical coating (400  $\mu\text{m}$ ), Ni barrier (50  $\mu\text{m}$ ), and carbon steel substrate after heat treatment at 1,100° C for 8 h. The region of interdiffusion essentially spanned the width of the Ni barrier, extending  $\approx 30 \mu\text{m}$  into the substrate and  $\approx 100 \mu\text{m}$  into the coating. A thinner diffusion barrier (25  $\mu\text{m}$ ) produced a similar diffusion profile.

Excellent adhesion of the alloy coating was exhibited when several samples were subjected to a standard bend test (20 pct elongation of the coating). All of the coatings were stressed until small cracks appeared on the surface, without showing any evidence of separation from the substrate. The coatings' adhesive properties appeared to be associated with the existence of an appreciable interdiffusion zone between the substrate and coating.

In the course of initial testing to determine the adhesive properties of the coating using bend test methods, it was observed that the 1020 steel substrate began to fracture before the coating did, as a result of its having lost a significant amount of ductility during heat treatment. Apparently, during the solution part of the annealing step, enough Cr and Ni diffused into the substrate to make it hardenable. When the coating was solution annealed, part

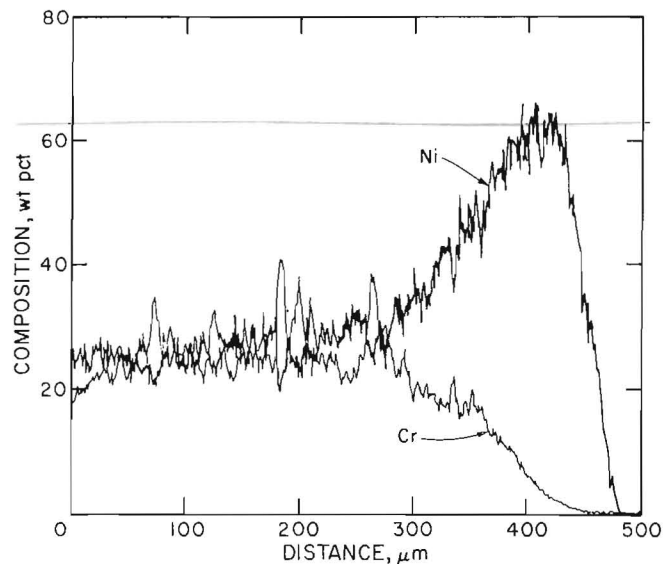


**Figure 11.**—Microprobe trace of heat-treated coating, showing the diffusion of Cr into the Ni undercoat and the inhomogeneity in the coating caused by incomplete diffusion of the occluded Cr powder.

of the substrate was transformed into untempered martensite. To restore the substrate to a more ductile structure, the coating and substrate were additionally tempered at 400° C for 4 h prior to the bend test. At this temperature, the interstitial stresses in the martensite were relieved without causing appreciable reprecipitation of carbides in the coating.

## Hardness and Ductility

The hardness of the alloy coatings was determined for several samples and related to their composition and microstructure as well as to the use of a diffusion barrier (table 3).

Hardness values obtained for nominal 77Fe8Ni15Cr alloy coatings, prepared both without and with a Ni diffusion barrier, were 1,650 and 154 DPH, respectively. Without the barrier, the hardness was 650 units greater than that of a typical quenched, martensitic 440C stainless steel (maximum 1.2 pct C). This would indicate that carbon diffused in from the substrate to produce a higher C level and therefore a harder martensite than 440C stainless steel. The highest hardnesses were observed nearer the substrate where the diffused carbon levels were higher. This hard, brittle martensitic coating was austenitized at 1,100° C for 1 h, cooled to 700° C, and held for 1 h to produce a ferritic 440C stainless steel having a hardness of only 186 DPH. With a 50- $\mu$ m-thick Ni barrier, the hardness value and the carbon concentration and microstructure were comparable to 304 stainless steel. A 330 type of stainless steel was produced simply by adjusting the composition of the electrolyte and the quantity of suspended Cr powder.

Electrodeposited alloys having the composition of a 330 stainless steel exhibited good ductility. Results of a series of standard bend tests conducted with eight alloy samples of this composition showed that the alloy could undergo 18-pct elongation before the initiation of fractures. This ductility is less than the 27- to 35-pct elongation determined for a Ni electrodeposit prepared from a Watts-type electrolyte (34) or the 30 pct required for 330 stainless steel (35) but more than the 2- to 3-pct elongation observed for a 60Ni40Fe alloy electrodeposited from a sulfate-chloride electrolyte (36).

## CORROSION RESISTANCE OF COATING

### Heat-Treatment Effects

The effectiveness of the heat-treatment procedure was measured by boiling the electrodeposited metal in 65-pct HNO<sub>3</sub> for five 48-h periods. This test (Huey test) was designed to identify Cr segregation in stainless steels. HNO<sub>3</sub> will preferentially dissolve those areas in the electrodeposit that have a lower Cr content. In conventional stainless steels, this is caused by localized chromium carbide precipitation at the grain boundaries.

Coatings containing ~55 pct Fe, 30 pct Ni, and 17 $\pm$ 1 pct Cr were physically removed from the cathode, vacuum heat treated at 1,100° C, and quenched in water. The coatings were removed from the substrate before heat-treating to eliminate the possibility of carbon diffusion from the substrate and to prevent the results of the test from being affected by the possible presence of pores that would allow the acid to attack the carbon steel substrate. The heat-treated coating was quenched to prevent localized chromium carbide precipitation.

Heat-treatment times of 4 to 16 h at 1,100° C produced low corrosion rates (table 4). The best corrosion resistance was obtained with a heat treatment of 8 h at 1,100° C.

Vacuum heat treatment is not required to obtain good corrosion rates. When the coatings were heat treated under a nitrogen atmosphere, there was no significant change in their corrosion rates.

## Protection of Carbon Steel

The integrity (protective quality) of the Fe-Ni-Cr alloy coating was demonstrated by exposing several substrate-plus-coating (43Fe36Ni21 $\pm$ 1Cr) specimens to the boiling 65-pct-HNO<sub>3</sub> solution. With a 50- $\mu$ m-thick Ni barrier and the electrolyte composition and heat-treatment conditions that had been established for producing a low-porosity, crack-free, homogenous alloy coating, a 250- $\mu$ m-thick coating protected the substrate during a 240-h test in the HNO<sub>3</sub> solution. Corrosion rates of 0.6 $\pm$ 0.4 mm/yr, with rates as low as 0.2 mm/yr, were obtained for the coated cathodes during these tests. Figure 12 illustrates the uniformity of corrosion of the coating after exposure to the acid environment.

## ELECTROFORMS

Because of the ability to deposit relatively thick (up to 750  $\mu$ m), deposits by this alloy coating method, its applicability to the preparation of electroforms (near-net-shape parts) showed excellent promise. A variety of small objects, including a 35-mL-capacity crucible as well as square and cylindrical shapes, were prepared on Sn-Bi alloy mandrels. The electroforms were removed from the mandrels, heat-treated to homogenize the metal, and quenched to prevent carbide segregation at the grain boundaries and the formation of eta phase (fig. 13). The electroforms can be polished to produce a smooth surfaced part in their final shape (fig. 14).

Table 3.—Cross-sectional microhardness and microstructure of Fe-Ni-Cr alloy coatings

Composition, wt pct				Barrier	Hardness, DPH	Microstructure observed	Comparable commercial alloy
Fe	Ni	Cr	C				
76	8	15	>1.2	None . . . . .	1,650 $\pm$ 500	Martensite . . . . .	440C stainless, quenched.
76	8	15	>1.2	.. do . . . . .	186 $\pm$ 60	Ferrite . . . . .	440C stainless, annealed.
77	8	15	<.2	Ni (50 $\mu$ m) . . .	154 $\pm$ 42	Austenite-ferrite. . . . .	304 stainless, annealed.
55	25	20	<.2	Ni (50 $\mu$ m) . . .	157 $\pm$ 42	Austenite . . . . .	330 stainless, annealed.

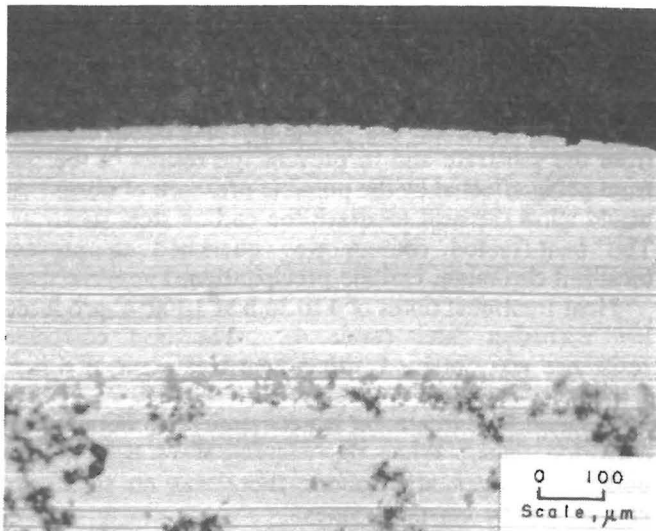


Figure 12.—Fe-Ni-Cr alloy coating after exposure to  $\text{HNO}_3$  solution.

Table 4.—Effects of heat-treatment time and furnace pressure on coating homogenization

Pressure, Torr	Time, h	Corrosion rate, mm/yr
$1 \times 10^{-6}$ .....	4	$4.1 \pm 1.3$
$1 \times 10^{-6}$ .....	8	$1.3 \pm 1.0$
$1 \times 10^{-6}$ .....	16	$4.0 \pm .7$
760 <sup>1</sup> .....	8	$2.0 \pm .5$

<sup>1</sup>Nitrogen atmosphere.

The results of 65-pct  $\text{HNO}_3$  corrosion tests conducted for 96 h on several 53Fe28Ni19Cr electroforms indicated good uniformity of alloy composition throughout the object. After four of the square- and crucible-shape objects were heat treated and each was cut vertically into half-sections, the average corrosion rate for the eight sections was  $1.0 \pm 0.6$  mm/yr. The corrosion rates of the two half-sections comprising each electroform were within 0.3 mm/yr of each other.

In addition to being used to produce electroforms, thick alloy coatings were also applied uniformly to threaded



Figure 13.—Heat-treated Fe-Ni-Cr alloy electroforms.

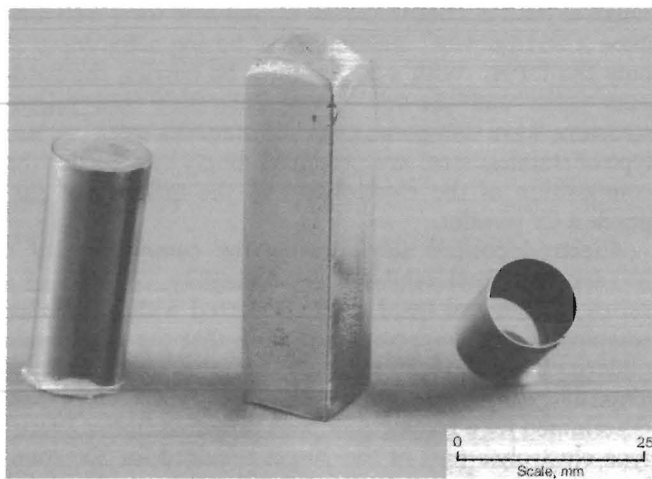


Figure 14.—Polished Fe-Ni-Cr alloy electroforms.

parts. A 440- $\mu\text{m}$ -thick coating can be plated on a coarsely threaded 1.27-cm-diam carbon steel rod. On the basis of this result, possibilities exist not only to prepare threaded electroforms but also to produce protective coatings on steel parts as substitutes for similar bulk stainless steel parts.

## CONCLUSIONS

Thick, Fe-Ni-Cr composite coatings have been deposited uniformly by a method in which suspended Cr particles are occluded into an electrodeposited Fe-Ni alloy matrix. The amount of Cr powder electrodeposited has been shown to be significantly affected by the amount of powder suspended in the plating bath, the composition of the Fe-Ni alloy matrix, the amount and type of surface active agents present, and the current density.

At present, coatings containing between 19 and 23 pct Cr powder can be consistently produced. There is still a

need, however, to improve understanding of the mechanism by which powders are incorporated into the Fe-Ni electrodeposit and the role of surface-active agents in the occlusion process.

Heat treatment of the metal-metal composite at 1,100° C for 8 h in an inert atmosphere or under vacuum sufficiently homogenized the coating to produce a corrosion-resistant coating. Shorter times did not homogenize the coating sufficiently to give optimum corrosion

resistance. Longer heat treatment did not improve the corrosion resistance of the coating.

Because the homogenized coating has a composition and microstructure similar to that of an austenitic stainless steel, quenching is required to prevent localized carbide precipitation at the grain boundaries and formation of eta phase and to preserve corrosion resistance. A 250- $\mu\text{m}$ -thick coating can be homogenized in an inert atmosphere

at 1,100° C for 8 h and quenched in water from 1,100° C to produce a defect-free coating capable of protecting a 1020 carbon steel substrate for 240 h in boiling 65-pct  $\text{HNO}_3$ . The corrosion rate of the coatings ( $0.6 \pm 0.4$  mm/yr) approaches the rate of 0.2 mm/yr exhibited by 304 stainless steel under similar conditions.

## REFERENCES

1. Celis, J. P., and J. R. Roos. Electrolytic and Electroless Composite Coatings. *Rev. Coat. and Corros.*, v. 5, No. 1-4, 1982, pp. 1-41.
2. Roos, J. R., and J. P. Celis. Is the Electrolytic Codeposition of Solid Particles a Reliable Coating Technology. Paper 0-1 in *Dispersion Coatings I (Tech. Proc. 71st Annu. Tech. Conf. Am. Electroplat. Soc., New York, July 16-19, 1984)*. *Am. Electroplat. Soc.*, Winter Park, FL, 1984, 14 pp.
3. Pushpavanam, N., G. Vardajan, S. Krishnamurthy, and B. A. Shenoi. Electrodeposited Composite Coatings. *Electroplat. & Met. Finish.*, v. 27, No. 5, 1974, pp. 10-15.
4. Sinha, P. K., N. Dhamansayan, and H. K. Chakrabarti. Electrodeposited Nickel-Alumina Compositions. *Plating*, v. 60, 1973, pp. 55-59.
5. Guglielmi, N. Kinetics of the Deposition of Inert Particles From Electrolytic Baths. *J. Electrochem. Soc.*, v. 119, 1972, pp. 1009-1012.
6. Roos, J. R., J. P. Celis, and H. Kelchtermans. Electrolytic Deposition of Copper Powders Containing a Dispersion of Fine Alumina Particles. *Powder Technol.*, v. 20, 1978, pp. 139-142.
7. Roos, J. R., J. P. Celis, and J. A. Helsen. Codeposition of Alpha- and Gamma-Alumina With Copper From Copper Sulphate Baths. *Trans. Inst. Met. Finish.*, v. 55, No. 3, 1977, pp. 113-116.
8. Buelens, C., J. P. Celis, and J. R. Roos. Electrochemical Aspects of the Codeposition of Gold and Copper With Inert Particles. *J. Appl. Electrochem.*, v. 13, 1983, pp. 541-548.
9. Brandes, E. A., and D. Goldthorpe. Electrodeposition of Cermets. *Metallurgica*, v. 76, Nov. 1967, pp. 195-198.
10. Foster, J., and B. Cameron. The Effect of Current Density and Agitation on the Formation of Electrodeposited Coating. *Trans. Inst. Met. Finish.*, v. 54, No. 4, 1976, pp. 178-183.
11. Snaith, D. W., and P. D. Groves. A Study of the Mechanisms of Cermet Electrodeposition. *Trans. Inst. Met. Finish.*, v. 50, No. 3, 1972, pp. 95-101.
12. Zahavi, J., and J. Hazan. Electrodeposited Nickel Composites Containing Diamond Particles. *Plat. and Surf. Finish.*, v. 70, No. 2, pp. 57-61.
13. Hassion, F., and J. Szanto. Occlusion of Diamond Dust in Chromium Plating on Steel. U.S. Army Weapons Command, Springfield, MA, SA-TRIS-1086, 1964, 27 pp.
14. Withers, J. C. Electroplated Cermet Coatings for Oxidation Protection of Substrates in Excess of 2,000° F (U.S. Air Force contract 33(616)-6807, Am. Mach. and Foundry Co.). *Wadd Tech. Rep.* 60-178, Jan. 1961, 75 pp.
15. Tomaszewski, T. W., L. C. Tomaszewski, and H. Brown. Co-Deposition of Finely Dispersed Particles With Metals. *Plating*, v. 56, 1969, pp. 1234-1239.
16. Zahavi, J., and H. Kerbel. Properties of Electrodeposited Composite Coatings as a Result of Their Formation Conditions. Paper D-3 in *General Session (Tech. Proc. 68th Annu. Tech. Conf. Am. Electroplat. Soc., Boston, MA, June 28-July 2, 1981)*. *Am. Electroplat. Soc.*, Winter Park, FL, 1981, 43 pp.
17. Narayan, R., and B. H. Narayana. Electrodeposited Composite Metal Coatings. *Rev. Coat. and Corros.*, v. 4, No. 2, 1981, pp. 113-155.
18. Young, J. P. Codeposition of Wear-Resistant Particles With Chromium. NBS, Washington, DC, NBSIR-74-615, 1976, 87 pp.
19. Celis, J. P., H. Kelchtermans, and J. R. Roos. Properties of Electrodeposited Copper-Alumina Coatings. *Trans. Inst. Met. Finish.*, v. 56, No. 1, 1978, pp. 41-45.
20. Sautter, K. F. Electrodeposition of Dispersion-Hardened Nickel- $\text{Al}_2\text{O}_3$  Alloys. *J. Electrochem. Soc.*, v. 110, 1963, pp. 557-560.
21. Greco, V. P., and W. Baldauf. Electrodeposition of Ni- $\text{Al}_2\text{O}_3$ , Ni- $\text{TiO}_2$ , and Cr  $\text{TiO}_2$  Dispersion Hardened Alloys. *Plating*, v. 55, 1968, pp. 250-257.
22. Tomaszewski, T. W., R. J. Clauss, and H. Brown. Satin Nickel by Co-Deposition of Finely Dispersed Solids. Paper in *Technical Proceedings of the 50th Annual Convention of the American Electroplaters' Society (Atlantic City, NJ, June 23-27, 1963)*. *Am. Electroplat. Soc.*, Newark, NJ, 1963, pp. 169-202.
23. Vest, C. E., and D. F. Bayzarre. Codeposited Nickel-Molybdenum Disulfide—A Self-Replenishing Solid Film Lubricant. *Met. Finish.*, v. 65, No. 11, 1967, pp. 52-58.
24. Bazzard, R., and P. J. Boden. Nickel-Chromium Alloys by Codeposition: Part I—Codeposition of Chromium Particles in a Nickel Matrix. *Trans. Inst. Met. Finish.*, v. 50, No. 2, 1972, pp. 63-69.
25. \_\_\_\_\_. Nickel-Chromium Alloys by Codeposition: Part II - Diffusion Heat Treatment of Codeposited Composites. *Trans. Inst. Met. Finish.*, v. 50, No. 5, 1972, pp. 207-210.
26. Kilgore, C. R. Engineered Composite Coatings. *Prod. Finish. (Cincinnati)*, v. 27, No. 8, 1963, pp. 34-40.
27. Williams, R. V. Electrodeposited Composite Coatings. *Electroplat. & Met. Finish.*, v. 19, No. 3, 1966, pp. 92-96.
28. Allison, J. E., Jr., and G. R. Smith. Alloy Plating Using a Particle Occlusion Method. Paper K-2 in *Alloy Plating I (Tech. Proc. 71st Annu. Tech. Conf. Am. Electroplat. Soc., New York, July 16-19, 1984)*. *Am. Electroplat. Soc.*, Winter Park, FL, 1984, 14 pp.
29. Smith, G. R., and J. E. Allison, Jr. Alloy Coating Method. U.S. Pat. 4,601,795, July 22, 1986.
30. Celis, J. P., and J. R. Roos. Kinetics of Alumina Particles From Copper Sulfate Plating Baths. *J. Electrochem. Soc.*, v. 124, 1977, pp. 1508-1511.
31. Fedorova, N. S. X-Ray Diffraction Structure Investigation of Electrodeposited Iron-Nickel Alloys. *Zh. Fiz. Khim.*, v. 32, 1958, pp. 1211-1213.
32. Tomaszewski, T. W. Effects of Anions on the Formation of Electrodeposited Composite Coatings: Some Experimental Evidence. *Trans. Inst. Met. Finish.*, v. 54, No. 1, 1976, pp. 45-48.
33. Million, B., J. Ruzickova, and J. Urestral. Diffusion in Fe-Ni-Cr Alloys With an FCC Lattice. *Mater. Sci. and Eng.*, v. 72, 1985, pp. 85-100.
34. Brenner, A., V. Zentner, and C. W. Jennings. Physical Properties of Electrodeposited Metals. I. Nickel. 3. The Effect of Plating Variables on the Structure and Properties of Electrodeposited Nickel. *Plating*, v. 39, 1952, pp. 865-894.
35. American Society for Testing and Materials. Standard Specification for Nickel Iron Chromium Silicon Alloy (UNS N08330 and N08332) Plate, Sheet, and Strip. B5336-83 in *1983 Annual Book of ASTM Standards: Volume 02.04, Nonferrous Metals-Nickel, Lead and Tin Alloys, Precious Metals, Primary Metals, Reactive Metals*. Philadelphia, PA, 1983, pp. 551-560.
36. Levy, E. M. Nickel-Iron Alloys Electrodeposited From Sulfate-Chloride Electrolyte: Effects on Mechanical Properties and Microstructure of Stress-Reducing Agent, Heat Treatment, pH, and Chemical Compositions. *Plating*, v. 56, 1969, pp. 903-908.